

# THE MANAGEMENT OF CHARACTERISTICS OF THE NEW TWO-LAYER RUBBER MATRIX SEALS

**Aslanov Jamaladdin Nuraddin**

*Department of Oil and Gas Equipment<sup>1</sup>  
camaladdin.aslanov@asoiu.edu.az*

**Abasova Sevinc Malik**

*Department of Engineering and Computer Graphics<sup>1</sup>  
seva-abasova@mail.ru*

**Huseynli Zenfira Seydi**

*Department of Oil and Gas Equipment<sup>1</sup>  
huseynli\_z@rambler.ru*

<sup>1</sup>*Azerbaijan State Oil and Industry University  
27 Azadliq str., Baku, Azerbaijan, AZ1010*

---

## Abstract

Rubber seals for closing devices operating in cold climates degrade quickly in aggressive environments at very low temperatures. As a result, leaks and failures occur in the closure devices. Therefore, there is a great need to develop a new model of rubber seals and develop their scientific basis.

The article is devoted to increasing the sealing effect of rubber seals of machines and equipment, including closures, by introducing the anisotropy of the rubber matrix into its structure with control of the characteristics of hard closures obtained from rubber. For this purpose, new models of the gate valve design were obtained and new models of two-layer panel seals based on a modified rubber elastomer matrix are applied to these structures.

For this, a test program is carried out in the form of an analytical trajectory of large, medium and small constant curves in two closed forms based on characteristic deformations to study the anisotropy of matrix deformations. It is found that the eigenvector of the deformation anisotropy of the matrix is not in the load trajectory before it collapses, it arises with a delay. This delay slows down the rate of destruction.

This property of deceleration of the main eigenvector of the deformation anisotropy of the matrix is subjected to a very complex loading of the initial fields, in the latter sections it is also observed in samples No. 2, 3, tested along the trajectory of linear loading. This delay slows down the destruction rate.

Thus, the direction of the deceleration property of the main eigenvector can be considered quite common. This leads to an increase in its resistance to wear in a highly aggressive environment.

**Keywords:** rubber matrix, anisotropy, matrix deformation, deformation trajectory, anisotropic matrix properties.

**DOI: 10.21303/2461-4262.2020.001401**

---

## 1. Introduction

There is a need to develop new types of sealing elements that can reliably operate on machines and equipment in various weather conditions around the world ( $-55^{\circ}\text{C}$  and  $+55^{\circ}\text{C}$ ). Even if to add the aggressiveness of the environment, the problem becomes even more complex. There is a great need for frost-resistant and heat-resistant rubber seals used primarily in equipment. This task requires the preparation of modern composite seals that work for mechanical wear (abrasive, water-jet and flammable) in highly corrosive environments.

When solving design problems and problems associated with changing the characteristics of the rigidity of rubber seals, rigid closures are often introduced into the rubber seal of the matrix, the deformation of which can be protected in comparison with the deformation of the matrix.

For this purpose, a new matrix model has been proposed for use in covering structures [1–3]. Therefore, by double matrixing, new rubber structural seals were used based on existing elastomer matrices based on the “Honeycomb Panel matrix” model. High-quality modified rubber elastomeric matrices of V-14 grade, 7130 grade, 7455 grade (Russian Federation) were subjected to the

“Honeycomb Panel matrix” model and new two-layer matrix panel seals were obtained [4–6]. Based on a two-layer matrix model, modern composite seals are resistant to freezing, heat, and wear in highly corrosive environments. These seals are adopted by the seals of the newly invented valve and can be applied to various types of closure devices.

As a real material, rubber can be viewed as the surface effect of the magnitude of anisotropy caused by inhomogeneous structure and diffusion microdamages, as well as the surface effects of the concentration of unavoidable stresses, considered in advance.

Information on the behavior of rubber seals in the matrix should be taken into account both when constructing a computational model for the destruction of a seal (rubber) and in the structural and technological improvement of rubber seals. When solving structural problems and problems with changing the characteristics of the rigidity of rubber seals, the deformation of the rigid closing elements of the rubber sealing matrix can maintain its resistance compared to the deformation of the matrix. When calculating the state of deformation of the rubber matrix, the boundary conditions of immobility and motion of coatings are taken into account. Therefore, only those coatings should be considered which are loose to a certain extent and their condition is determined by the deformation state of the rubber matrix. From this point of view, for example, hardening of solid binders is carried out by the method of fiber reinforcement [7–10].

Predicting the performance of high-quality modified rubber elastomeric matrices B-14 [5], exposed in the model “Honeycomb Panel matrix” (Greece) to new two-matrix panel seals, by studying the deformation under stress [6].

The performance of the modified rubber elastomeric matrices of the B-14 brand was confirmed in an aggressive environment at a temperature (–55 °C) [5]. *The aim of research* is to ensure an increase in the resistance of the new matrix to mechanical forces by introducing rigid cover plates into the matrix [6]. Therefore, the tests carried out in the study (–10 °C) were also carried out inside the petroleum product.

## 2. Materials and methods of research

The prediction of the stress fracture of rubber reinforcement by fiber-loaded solid gates assumes information about the breaking stresses and limiting deformations of all individual fibers. Since rubber seals with reinforced ceilings are characterized by the same limiting stresses and deformations, some of the characteristic features of the behavior of rubber seals, which are well confirmed by experiment, can be realized. In addition, the influence of the characteristics of the matrix and the conditions under which the fibers actually strengthen the matrix are considered. This state is more easily taken into account if one of them has limiting deformations. And the strength of the reinforcement is determined by the fibers as the maximum stress, i. e. the maximum load is related to the initial cross-sectional area of the seal specimen.

Real materials are never homogeneous, and rubber with different overlaps already has a certain level of strain anisotropy matrix. Anisotropy is caused by both structural heterogeneity and diffuse microdestruction [7–10]. In this case, using variations of ways to minimize potential energy, the latter is defined as the sum of the corresponding energy-deformation of the rubber matrix (seal)  $\Pi$  [8, 9], counted within the volume and compression energy of the inclusion of filaments:

$$\Phi = \Pi + \frac{1}{2} \int_0^{L_k} E_k \left( \frac{\partial u_k}{\partial s} \right)^2 ds, \quad k = 1, 2, \dots, N, \quad (1)$$

where  $k$  – the number of fibers,  $L_k$  – the length of the fiber; “ $u_k$ ” – offset along the fiber;  $E_k$  – elastic modulus of the fiber.

In this formulation, applying the Ritz method [8], the total displacement field “ $u_k$ ” in “ $u_k$ ” is determined and the simple value “ $u$ ” of the fiber coordinates is determined. On trajectories of constant curvature, the dependence of the elastic constants included in eq. (1) and the strain anisotropy matrix at the arc length  $S_0$  and curvature, and the load trajectory  $\chi$  is studied experimentally. Improved accuracy is achieved by combining fiber trajectories with element connections and especially with fiber ends with knot points. The experiments were carried out along a trajectory in the

form of two-section dashed lines, where a series of samples is displayed. For each of the 8 series, one natural sample was prepared and tested. These patterns are numbered from 1 to 8.

Deactivation of rubber occurs by compression of the seal in the leading cylindrical shells. Compression occurred until those deformations, after which the further program of trajectories was studied. The trajectory consists of straight lines of various slopes (signs of the seal deformation), the dependence of the elastic constants, and the deformation of the matrix anisotropy along the arc length  $\sigma_g$  and the inclined angle  $\theta$  of the trajectories.

Partial unloading was carried out during tests at different points of each loading trajectory. Unloading is carried out in two different directions of the same trajectory to the next unloading point. Thus, measurements were obtained separately for each sample during unloading at different points of the trajectory, which makes it possible to reliably compare the data obtained.

In particular, two samples were tested on the following trajectories: the trajectory of constant curvature, accompanied by compression until the depletion of the delay sign [5], after which the trajectories differed at an angle of  $75^\circ$  relative to the stress vector. As a result, experimental data were obtained for constructing the deformation anisotropy of the matrix for indicating load trajectory recorders.

In this case, based on the instructions, stress components  $\sigma_1, \sigma_3$  were calculated on strain-gauge recorders (devices) of complex loading  $\sigma_1 - E_{11}$  and [8, 9]  $\sigma_3 - E_{13}$ , and strains components  $\sigma_1, \sigma_3$ , and deformation  $E_{11}, E_{13}$  and vector components of stress increments corresponding to the unloading process were determined. In all cases, during unloading, a compaction matrix is formed, which has only the initial values of the elastic modulus.

The elastic modulus or the coefficients of the strain anisotropy matrix  $E_{mn}$  were determined for the plane stress condition, i. e. with constant curvature and in the form of two-link broken lines, based on the fact that curvatures are constant; and – the number of elastic constants is three. The three coefficients of the strain anisotropy matrix  $E_{mn}$  are expressed as three elastic constants  $S_{ij}^*$  (where  $S_{ij}^*$  is the function of hydrostatic stress).

The strain anisotropy matrix coefficients  $E_{mn}$  are expressed in the form of two elastic constants:  $P_k, N_k$  or  $S, S_{11}$  (the components of the hydrostatic stress function are in vector form). Hence, determined experimentally, these two elastic constants are calculated for the elastic anisotropy parameter. Therefore, in this case, based on Hooke's law, any elastoplastic load will be as follows:

$$\begin{aligned}\Delta\sigma_1^{(P)} &= E_{11}\Delta E_{11}^{(P)} + E_{13}\Delta E_{13}^{(P)}, \\ \Delta\delta_3 &= E_{13}\Delta E_{11}^{(q)} + E_{33}\Delta E_{13}^{(q)}.\end{aligned}\quad (2)$$

The strain anisotropy matrix coefficients  $E_{11}, E_{22}, E_{33}$  are determined directly. Here  $P=1.2$  and  $q=1$  or  $2$  (or vice versa  $q=1.2$  and  $P=1$  or  $2$ ), depending on which component prevails during unloading.

Since the increments  $\Delta\sigma_1, \Delta\sigma_3$  and,  $\Delta E_{13}$  are directly measured on a device (tensometer), and then the coefficients of the strain anisotropy matrix will be determined with the accuracy of the experiment [8, 9].

It should be noted that the coefficient of the deformation anisotropy matrix for any characteristic trajectories will be determined by systems of equations (2) in the future by the formulas

$$E_{11} = \frac{\Delta_1^*}{\Delta^*}, \quad E_{13} = \frac{\Delta_2^*}{\Delta^*}, \quad E_{33} = \frac{\Delta_3^*}{\Delta^*}, \quad (3)$$

where  $\Delta^*$  – determinant of the system,  $\Delta_i^*$  are the determinants obtained by  $\Delta^*$  replacing the elements with the corresponding free terms.

### 3. Research results

**Table 1** shows the values of the coefficients for samples No. 1–3, calculated by the formula (2). These samples (rubber seals with reinforced inclusions), relatively, along the trajectories of

small ( $\chi=148$ ), medium ( $\chi=250$ ) and large ( $\chi=500$ ) curvatures  $\chi$ . **Table 1** shows that the coefficient  $E_3$  essentially depends on the curvature, while the coefficient  $E_{11}$  is independent or in any case depends on it less weakly. Using the indicated data, the approximating straight lines are chosen by the method of less squares:

$$E_{33} = (2.548 - 12.2 \cdot S_0) \cdot 10^6. \quad (4)$$

For sample No. 1 ( $\chi=148$  – small curvature trajectory);

$$E_{33} = (2.949 - 18.8 \cdot S_0) \cdot 10^6. \quad (5)$$

For sample No. 2 ( $\chi=250$  – medium curvature trajectory);

$$E_{33} = (3.377 - 52.7 \cdot S_0) \cdot 10^6. \quad (6)$$

For sample No. 3 ( $\chi=500$ ) – large curvature trajectory), where the coefficient  $E_{33}$  has the size (MPa).

It should be noted that the approximation of the experimental points for sample No. 2 must be performed with respect to a square polynomial. But it should be borne in mind that the experimental points for samples No. 1 and No. 3 are located near a straight line, and allowing a certain error associated with the implementation of the program along a trajectory of large curvature, the approximating curve is drawn along a straight line.

As can be seen from dependence (4)–(6), free terms ( $a_0$ ) and coefficients for  $S_0$  ( $a_1$ ) essentially depend on the curvature. Thus, in this case, there are approximating lines.

$$E_{33} = a_0^q - a_1^q S_0, \quad q = 1, 2, 3, \quad (7)$$

where  $a_0 = a_0(\chi)$  and  $a_1 = a_1(\chi)$  i. e. are functions of curvature and load trajectory.

$$a_0 = (1.734 - 64.3\chi - 625\chi^2) \cdot 10^6, \quad (8)$$

$$a_1 = (0.937 - 10.9\chi + 1,940\chi^2) \cdot 10^6. \quad (9)$$

**Table 1**

The values of the coefficients for samples No. 1–3, calculated by the formula (2)

Sample No., tester type	Unloading arc length $S_0, 10^{-4}$	$E_{11} \cdot 10^5$ MPa	$E_{13} \cdot 10^5$ MPa	$E_{33} \cdot 10^5$ MPa
No. 1	48.8	2.02	−0.037	2.54
	78.9	2.07	−0.018	2.42
	106.1	2.01	−0.088	2.42
	180.4	1.92	−0.056	2.43
	21.1	2.03	−0.171	2.84
No. 2	40.4	2.29	−0.109	2.93
	58.5	1.98	0.108	2.81
	118.2	2.03	0.067	2.28
	22.1	2.46	−0.084	3.66
	36.7	2.18	0.137	2.84
No. 3	75.2	1.89	−0.023	2.88
	88.6	2.13	0.236	2.74
	118.1	1.36	0.343	2.98

The coefficients of the least squares matrix for the curvature values  $\chi$  are equal to 148, 250, 500. Thus, the coefficient of the strain anisotropy matrix  $E_{33}$  is a function of the curvature  $\chi$  and the arc length  $S_0$  is the load trajectory:

$$E_{33} = a_0(\chi) - a_1(\chi) \cdot S_0, \quad (10)$$

where  $a_1$  and  $(\chi)$  are respectively determined by formulas (8) and (9).

The retarding properties of the main eigenvector of the deformation-anisotropy-compaction matrix are determined by stops. Strain anisotropy matrices (square matrix of the second order)  $E=(E_{mn})$  define a linear map of a two-dimensional vector plane over a real field or complex numbers in itself.

**Fig. 1** shows the second order approximating polynomials.

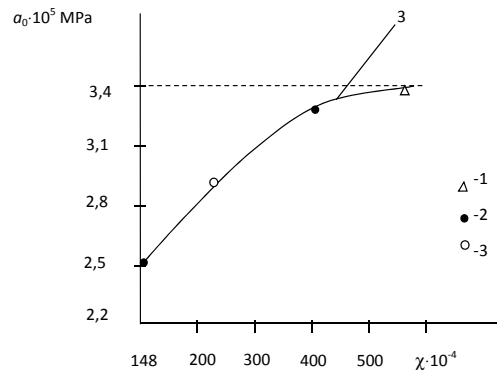


**Fig. 1.** Dependence of  $a_0$  on curvature:

1 – sample No. 1 ( $\chi=148$ ); 2 – sample No. 2 ( $\chi=150$ ); 3 – sample No. 3 ( $\chi=500$ )

In the plane  $El_1, El_3$ , relatively, a certain specified mapping is associated with a vector  $\overline{El}$  with vector coordinates  $El_1, El_3$  with coordinates  $\sigma_1, \sigma_3$  by means of relations [8, 9].

A relatively definite image shown in the plane  $El_1, El_3$  is associated with a vector  $\overline{El}$ , vector coordinates  $El_1, El_3$  and coordinates  $\sigma_1, \sigma_3$  i. e. is associated with the given relations in formula (7).

$$\sigma_i = E_{i,j} El_j, \quad (i, j = 1, 3), \quad (11)$$

which can be written as vector-matrix symbology

$$\overline{\sigma} = E \overline{El}. \quad (12)$$

For a square matrix of the second order  $E=(E_{mn})$  the problem can be solved to find nonzero vectors  $El$  and  $El_n$ , which are collinear in the image  $E$ . The problem is reduced to finding a vector  $El$  so that,

$$E \overline{El} = \lambda El \quad (13)$$

or

$$(E - \lambda J) \overline{El} = 0. \quad (14)$$

For this equation to have a nonzero solution, it is necessary and sufficient that the matrix  $E - \lambda J$  is unique. For this  $\lambda$  must be the root of the characteristic equation.

$$f(\lambda) = 0, \quad (15)$$

where  $f(\lambda)$  is the characteristic polynomial:

$$f(\lambda) = \begin{vmatrix} E_{11} - \lambda & E_{13} \\ E_{13} & E_{33} - \lambda \end{vmatrix}, \quad (16)$$

so that

$$f(\lambda) = \lambda^2 - (E_{11} - E_{33})\lambda + E_{11}E_{33} - E_{13}^2. \quad (17)$$

If  $\lambda$  is any zeros of this polynomial, then the equation will be

$$(E - \lambda J)\overline{El} = 0 \quad (18)$$

have nonzero matrix solutions  $El$ , the root of the characteristic equation is called the characteristic numbers of the matrix  $E$ , the corresponding solutions  $El$  are correct solutions and the vectors are eigenvectors. It is known that the characteristic polynomial is invariant with respect to coordinate transformation. Consequently, the roots of the characteristic equation are invariant under linear transformations. Using equation (15), the characteristic roots  $\lambda_1, \lambda_2$  of the strain anisotropy matrix are found:

$$\lambda_{1,2} = \frac{1}{2} \left( E_{11} + E_{33} \pm \sqrt{(E_{11} - E_{33})^2 + 4E_{13}^2} \right). \quad (19)$$

Solving the equation,

$$(E_{11} - \lambda)El_1 + E_{13} \cdot El_3 = 0, \quad E_{11}El_1 + (E_{33} - \lambda)El_3 = 0. \quad (20)$$

Two eigenvectors of the matrix  $(E_{mn})$  are found for  $\lambda = \lambda_1$  and  $\lambda = \lambda_2$ . For  $\lambda = \lambda_1$  and  $\lambda = \lambda_2$ , the determinant of system (20) disappears, and in this case one of the coordinates, for example,  $El_3$ , takes arbitrary values:

$$El_1 = -\frac{E_{13}}{E_{11} - \lambda} \cdot El_3, \quad El_1 = -\frac{E_{33} - \lambda}{E_{13}} \cdot El_3. \quad (21)$$

For  $\lambda = \lambda_1$  and  $\lambda = \lambda_2$  (21), a pair of orthogonal eigenvectors of the matrix  $(E_{mn})$  is determined. In **Fig. 2, 3**, for samples No. 4–8, tested for  $s_0 = 1.2$  and 2.14, respectively, measurements of the proper location of the deformation anisotropy matrix of a seal with inclusions are shown relative to the load trajectory.

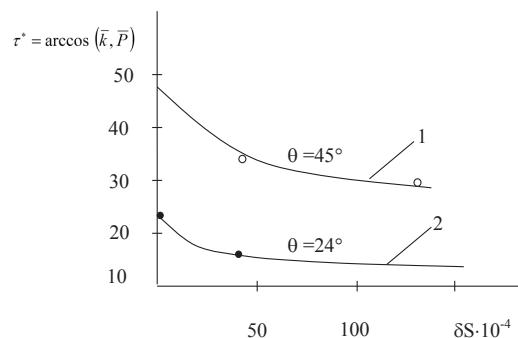


**Fig. 2.** The change in the eigenvector relative to the loading trajectory is 1.2 %:  
1 – sample No. 4; 2 – sample No. 5

In these graphs, a value  $\tau^*$  equal to  $\arccos(\bar{k}, \bar{p})$  is plotted along the ordinates that determine the inclination angle of the eigenvector to the load trajectory. Here  $\bar{k}$  is the unit vector directed along the trajectory (**Fig. 4**) and  $\bar{p}$  is the unit vector characterizing the direction of the eigenvector of the anisotropy matrix of the compaction deformation with stops.

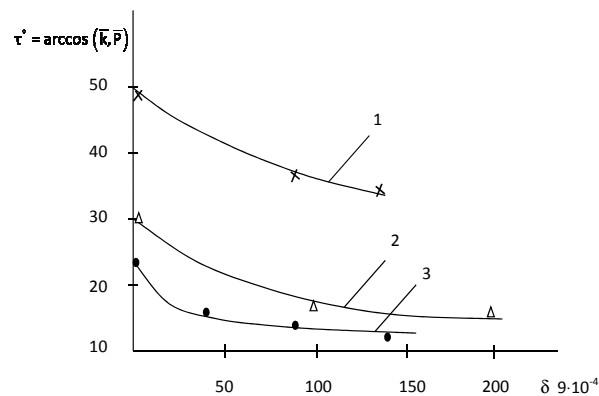


**Fig. 3.** Change in the correct loading trajectory by 2.1 %:  
1 – samples No. 6; 2 – samples No. 7; 3 – samples No. 8

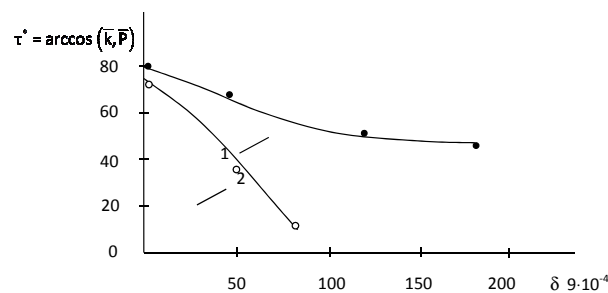


**Fig. 4.** Change the correct loading trajectory to slow down:  
1 – samples No. 2; 2 – samples No. 3

From **Fig. 4** it can be seen that with an increase in the arc length  $\delta s$ , the direction of the eigenvector of the strain anisotropy matrix tends to the direction of the load trajectory, i. e. in this case there is a deceleration property.

After processing the results obtained, it is determined that the eigenvector of the deformation anisotropy of the matrix is not found immediately after fractures on the loading trajectory, it appears with a delay. This property of deceleration of the main eigenvector of the deformation anisotropy of the matrix is subjected to a very complex loading of the initial fields, in the latter sections it was also observed in samples No. 2, 3, tested along the trajectory of linear loading (**Fig. 5**). This delay slows down the rate of destruction.

Thus, the direction of the deceleration property of the main eigenvector can be considered quite common. This leads to an increase in its resistance to wear in a highly aggressive environment.

#### 4. Discussion of research results

Based on expressions (3)–(7), from those calculated in **Table 1** values, it is possible to say that “the introduction of rigid closures into the rubber matrix creates a retarding property of the main special vector of the matrix deformation during its loading.

From expression (21) and **Fig. 4, 5** it can be seen that with an increase in the length of the axis, the direction of the special anisotropy vector of the matrix deformation tends to the direction of the loading trajectory. In this case, the deceleration property proves its existence.

When solving the problem, a special pair of orthogonal matrix vectors was defined. In **Fig. 2, 3**, for samples No. 4–8, respectively, tested at  $s_0=1.2$  and  $2.14$ , the deformation anisotropy of the seal matrix along the load trajectory was measured. Based on these measurements, in the graphs, the exponent  $\tau^*$ , which is equal to  $\arccos(\bar{k}, \bar{p}) - \alpha$ , is plotted on the length of the ordinate, which determines the angle of curvature in the load trajectory of the special vector.

The results show that with an increase in the axis length  $\delta s$ , the direction of the special anisotropy vector of the matrix deformation tends to the direction of the loading trajectory. That



is, in this case, the deceleration property appears. This deceleration is accompanied by load resistance (Fig. 5).

Based on this property, it is possible to say that indeed «by introducing rigid closures into the rubber matrix, it is possible to increase its load stability».

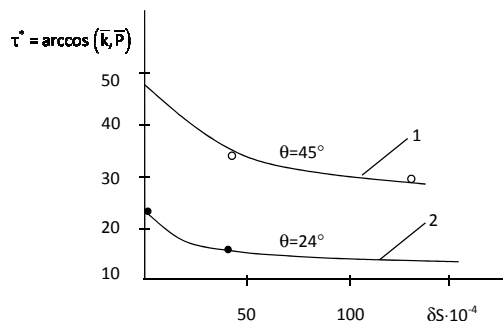


**Fig. 5.** The change in the eigenvector relative to the loading trajectory is 1.2 %:  
1 – sample No. 4; 2 – sample No. 5

The research is based on theoretical and experimental study of the reaction of the new model of rubber seals with a double matrix to stress deformation. The main approach of the study is to determine the pattern of change with computer simulation of the degree of deformation depending on the force, which is one of the important issues when choosing a seal cell.

The processing of the research results shows that there are limiting stresses and deformations in reinforced coated rubber seals. In addition, the condition that the fibers actually strengthen the matrix characterizes that one of the fibers has a limiting deformation. This reinforced strength is defined as the maximum stress in the fibers, that is, the maximum load is related to the initial cross-sectional area of the seal sample. This relationship is shown in Fig. 6. Real materials are never homogeneous, and various coated rubbers already have a certain matrix level of deformation anisotropy.

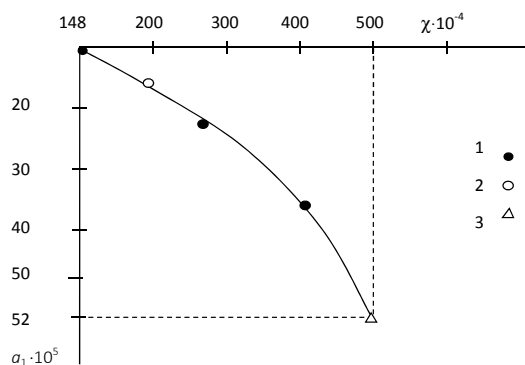


**Fig. 6.** Dependence  $a_1$  on thickness:  
1 – sample No. 1 ( $\chi=148$ ); 2 – sample No. 2 ( $\chi=150$ ); 3 – sample No. 3 ( $\chi=500$ )

The results obtained show that the new model of two-layer matrix seals is stable in the process of obtaining and uniform distribution of force and in the process of deformation against the force relative to existing seals. It can be used in all machines and equipment where it is necessary to prevent leakage between metal-to-metal surfaces. New valves provided by these seals have been developed and tested within the framework of the project of the Azerbaijan State University of Oil and Industry.

In the future, research will be carried out to determine the change in the regularity of the degree of deformation depending on the force using computer simulations, the choice of the seal cell depending on the deformation.



## 5. Conclusions

Studies have shown that the prediction of failure of fiber-loaded rigid binders depends on the breaking stresses and ultimate deformations of all other fibers. The condition that the introduced fibers actually strengthen the matrix is taken into account as its characteristic in the event that one of them has a limiting deformation, and the strength of the reinforcement  $\sigma_c$  in the fibers is determined as the maximum stress.

The experiments were carried out with a trajectory consisting of two-section broken lines. Here is a series of examples. For each of the 8 series, one natural sample was prepared and tested. The tests were carried out on each sample.

The anisotropy strain coefficients  $E_{mn}$  of the matrix are expressed by two elastic coefficients  $P_k, N_k$  or  $S, S_{11}$  (the components of the hydrostatic stress of the function are in the form of a vector). And also on the basis of the elastic-plastic load for the parameters of elastic anisotropy, the coefficients of deformation anisotropy  $E_{11}, E_{13}, E_{33}$  for samples No. 1–3 were calculated and the data obtained are given in **Table 1**.

In the tested samples of the seal No. 2, 3, the deceleration property of the main special vector of the deformation anisotropy of the matrix was revealed. Although the sections were subjected to very complex loading in the beginning, a linear loading trajectory was observed in the end sections. This delayed linear load slows down the rate of destruction. As a result, the stability of the seal is increased.

Expressions (19) and (21) were obtained to determine a special pair of orthogonal matrix vectors. Based on this special pair of vectors, experiments were carried out for samples 4–8. Accordingly, these samples were used to measure the anisotropy of the deformation of the sealant matrix along the loading trajectory and the dependence was established (**Fig. 2, 3**).

It can be seen from the graphs that with an increase in the length of the  $\delta s$  axis, the direction of the special anisotropy vector of the matrix deformation tends to the direction of the loading trajectory, i. e. in this case, the deceleration property is formed.

---

## References

- [1] Wahl, L., Maas, S., Waldmann, D., Zürbes, A., Frères, P. (2012). Shear stresses in honeycomb sandwich plates: Analytical solution, finite element method and experimental verification. *Journal of Sandwich Structures & Materials*, 14 (4), 449–468. doi: <https://doi.org/10.1177/1099636212444655>
- [2] Krzyżak, A., Mazur, M., Gajewski, M., Drozd, K., Komorek, A., Przybyłek, P. (2016). Sandwich Structured Composites for Aeronautics: Methods of Manufacturing Affecting Some Mechanical Properties. *International Journal of Aerospace Engineering*, 2016, 1–10. doi: <https://doi.org/10.1155/2016/7816912>
- [3] Zhang, Q., Yang, X., Li, P., Huang, G., Feng, S., Shen, C. et. al. (2015). Bioinspired engineering of honeycomb structure – Using nature to inspire human innovation. *Progress in Materials Science*, 74, 332–400. doi: <https://doi.org/10.1016/j.pmatsci.2015.05.001>
- [4] Aslanov, J. N. (2017). Valve, Useful model. State Standardization Metrology Agency for Pat. No. U20160018. Official bulletin, 7.
- [5] Davydova, M. L., Haldeeva, A. R. (2014). Modifikatsiya reziny na osnove butadien-nitril'nogo kauchuka termorasshirennym grafitom. *Himiya: Obrazovanie, nauka, tekhnologiya. Sbornik trudov vserossiyskoy nauchno-prakticheskoy konferentsii s elementami nauchnoy shkoly*. Yakutsk, 265–270. Available at: <https://www.elibrary.ru/item.asp?id=22436979>
- [6] Aslanov, J. N. (2020). New model rubber matrix for connectors application of sealers. *Equipment. Technologies. Materials*, 3, 16. Available at: <http://emtaso.ru/index.php/en/2-uncategorised/80-new-model-rubber-matrix-for-connectors-application-of-sealers>
- [7] Nuraddin, A. J., Baxman, S. A. (2018). Forecasting of Improved Straightforward Valves Technical Condition Using Fuzzy Inference Models. *IFAC-PapersOnLine*, 51 (30), 12–14. doi: <https://doi.org/10.1016/j.ifacol.2018.11.236>
- [8] Mamedov, V. T., Mamedov, G. A., Aslanov, J. N. (2020). Stress-Strain State of Sealing Rubber Membranes at Large Deformations. *Journal of Applied Mechanics and Technical Physics*, 61 (2), 286–291. doi: <https://doi.org/10.1134/s0021894420020157>
- [9] Shear modulus, G. (2019). IUPAC Compendium of Chemical Terminology. doi: <https://doi.org/10.1351/goldbook.s05635>
- [10] Nuraddin, A. J., Baxman, S. A., Abulfas, H. I. (2019). Model Design For Predicting The Efficiency Of Improved Valve Constructions During Statistical Data Based Exploitation. *IFAC-PapersOnLine*, 52 (25), 547–550. doi: <https://doi.org/10.1016/j.ifacol.2019.12.603>

Received date 02.07.2020

Accepted date 26.08.2020

Published date 30.09.2020

© The Author(s) 2020

This is an open access article under the CC BY license  
(<http://creativecommons.org/licenses/by/4.0>).